Open Journal of Earthquake Research, 2026, 15(4), 75-97
https://www.scirp.org/journal/ojer
ISSN Online: 2169-9631
ISSN Print: 2169-9623

Earthquake Forecasting by Lunar-Solar Dynamics

Michael John Leigh Chapman

Independent Researcher, Paranaque, Philippines
Email: earthtremors.org@gmail.com

How to cite this paper: Chapman, M.J.L. (2026) Earthquake Forecasting by Lunar-Solar Dynamics. *Open Journal of Earthquake Research*, **15**, 75-97.
https://doi.org/10.4236/ojer.2026.154004

Received: August 4, 2026
Accepted: September 14, 2026
Published: September 17, 2026

Abstract

This paper presents an analysis for earthquakes in 3 regions, including Asia Pacific (AP), Americas (AM) and Europe-Africa (EA), with Asia-Minor and relations with lunar/solar orbit data over the last approximately 17 years, with a view to enabling reliable earthquake forecasts. The evidence indicates a complex relationship between Earth, Moon, and Sun is largely responsible for the timing of earthquakes. The understanding of the lunar and solar orbit as a major influence is key to accurate advance prediction of earthquakes on an hourly basis. The method relies on correlation of historic solar-lunar geo-spatial criteria occurring simultaneously with significant quake events with known location and time of occurrence to within 1 hour, with projections based on expected lunar-solar geo-spatial criteria based on established computations. Results of analyses carried out between July 2023 and June 2024 indicate that for AP about 63% of actual events had effective forecasts, while for AM about 76% of actual events had effective forecasts. The effectiveness for EA was lower at 45%. Although far from foolproof, these techniques represent a step towards providing meaningful real-time short-term forecasts for earthquakes in all parts of the world.

Keywords

Earthquake, Hourly Forecasts, Lunar-Solar Dynamics, Historic Correlation

1. Introduction

The present paper has been written to introduce the idea of lunar-solar dynamics as a tool for prediction of earthquakes on an hourly basis. The method is simple in concept and does not require large AI-type support, so is relatively environmentally friendly. Although previous papers have suggested that use of Earth tide models could be a solution to prediction of earthquakes, development of this approach appears to be slow. The lunar-solar dynamics approach has been around for many years now, but has not been recognized as successful due partly to unclear presentation in earlier papers. It is therefore hoped that the present paper will break through the earlier confusion and lead to acceptance that there is room for further development of this method.

With respect to recent advances mainly due to benefits of electronic sensing equipment, the following are noted as being relevant:

Referring to an article [1] by Robert J Geller in Geophysical Journal International, Volume 131, Issue 3, December 1997, "Earthquake prediction research has been conducted for over 100 years with no obvious successes. Claims of breakthroughs have failed to withstand scrutiny. Extensive searches have failed to find reliable precursors. Theoretical work suggests that faulting is a non-linear process which is highly sensitive to unmeasurably fine details of the state of the Earth in a large volume, not just in the immediate vicinity of the hypocenter. Any small earthquake thus has some probability of cascading into a large event. Reliable issuing of alarms of imminent large earthquakes appears to be effectively impossible."

In their October 2004 paper [2]: "Earth Tides Can Trigger Shallow Thrust Fault Earthquakes", authors: Elizabeth S. Cochran, John E. Vidale, Sachiko Tanaka showed a correlation between the occurrence of shallow thrust earthquakes and the occurrence of the strongest tides. Their results also quantified the effects of applied stress on earthquake triggering, a key factor in understanding earthquake nucleation and cascades whereby one earthquake triggers others.

In his November 2005 article [3]: "Testing earthquake prediction methods: 'The West Pacific short-term forecast of earthquakes with magnitude MwHRV ≥ 5.8'", author V.G. Kossobokov has referred to the requirement for an exact definition of the anticipated phenomenon and the rules which define clearly in advance of it whether the prediction is confirmed or not. He has cited the proposed 1976 definition by the distinguished Panel on Earthquake Prediction, according to which: "An earthquake prediction must specify the expected magnitude range, the geographical area within which it will occur, and the time interval within which it will happen with sufficient precision so that the ultimate success or failure of the prediction can readily be judged. Only by careful recording and analysis of failures as well as successes can the eventual success of the total effort be evaluated and future directions charted. Moreover, scientists should also assign a confidence level to each prediction." The present analysis has taken account of much of the above proposals, although confidence limits have not yet been assigned, pending a more thorough analysis of statistical dependence. The present analysis has a main weakness that the magnitude range of events is presently defined by the lower limit (M4+) only.

Research into earthquake prediction has come a long way since the above. In the journal [4], Soil Dynamics and Earthquake Engineering, Volume 200, Part A, January 2026, 109740, Ranking Earthquake Prediction Algorithms: A Comprehensive Review of Machine Learning and Deep Learning Methods has been presented by authors Alireza Moghadamnejad, Mohammad Amin Moghaddasi, Mohammadjavad Hamidia, Reza Karami Mohammadi and Mehdi Zare. "Machine Learning (ML) has revolutionized earthquake prediction by significantly enhancing its predictive accuracy and analytical capabilities. In contrast to conventional seismological techniques that depend on fixed statistical models and geological assessments, machine learning enables the processing of extensive datasets to detect intricate, non-linear patterns embedded within seismic activity. Despite these achievements, challenges persist, including data sparsity, the uneven distribution of seismic records, and the inherent complexity of geological processes. Nevertheless, continued interdisciplinary collaboration and technological innovation are expected to drive further progress in the field, contributing to more reliable and actionable earthquake prediction systems."

From the above reference, spatiotemporal processes in earthquake prediction are made, which focus on analyzing seismic activity across spatial and temporal dimensions to uncover patterns and predict future events. These methods combine spatial data, such as fault line distributions and tectonic stress zones, with temporal information, including recurrence intervals and seismic cycles. Advanced techniques, such as statistical models, machine learning, and geophysical observations, are employed to study phenomena like earthquake clustering, aftershock sequences, and fault interactions. There is reference to Zhang *et al.* [5], who introduced a deep learning-based approach for earthquake prediction that addresses the constraints of localized models by integrating both temporal and spatial correlations at a global level. The experimental outcomes of this work revealed that the approach achieved an average recall of 51.83% and precision of 64.54% on test data. Interesting work has also been carried out [6] by M. Yousefzadeh, S.A. Hosseini and M. Farnaghi with earthquake prediction using a deep neural network using three selected pixels in Iran to predict the magnitude of earthquakes in the next 7 days using multiple (16) seismic parameters. The results appeared to be highly successful with a Positive Predictive Value (PPV) of 87.9% for higher earthquake classes (M5+).

Also from the above reference, Astuti *et al.* [7] integrated Earth's electric field data through Singular Value Decomposition (SVD) with the Support Vector Machine (SVM) classifier to predict upcoming earthquakes. This approach achieved 77% accuracy in predicting the location and 67% in forecasting future earthquakes' magnitude. Additionally, their method provided time predictions for earthquakes with magnitude 5 occurring two days in advance and magnitude 6 events predicted seven days in advance. Rafiei and Adeli [8] attempted to predict the magnitude and location of an earthquake weeks in advance in California. They employed Cellular Automaton to assess the likelihood of an earthquake surpassing a predefined magnitude threshold within a given period. Additionally, a mathematical optimization algorithm was used to identify the location with the highest probability of the earthquake occurring.

The above paragraphs indicate that there is growing interest in the field of earthquake prediction using machine learning techniques, but this may be distracting authors from using traditional analytical methodologies.

The Earth's crust and tectonic plates can be compared to a fractured eggshell on a softly boiled egg. Force applied to any part of the surface area will result in distortion of the egg and movement of the shell fragments. The Earth's crust is in equilibrium with its adjoining environment. Any disruption of this equilibrium, whether by lunar forces, nuclear explosions, change of state from ice to water (through global warming), internal thermal convection or geomagnetic forces, or change in differential atmospheric pressure across plate boundaries, may result in catastrophic imbalance and increased earthquake and volcanic activity.

The author's first approach was to relate earthquake events to lunar factors on a direct statistical basis. However, based on the long-term analysis, it appeared that there was little if any consistent influence of the Moon on earthquakes, as these seemed to occur at a range of phases and at all times of day.

More recent analysis (since late 2008) has been made which takes account of the lunar/solar orbits on an hourly basis. In retrospect, not surprisingly, it has determined that the spatio-temporal vector of the orbiting Moon and the Sun at any given moment with respect to each tentative earthquake zone is of paramount importance. The main lunar effect is tangential pulling of the tectonic plates when the Moon is close to the horizon. However, the sun, which has an effective tidal pull of slightly less than half that of the moon, also plays a decisive role in triggering quakes, as its force adds or subtracts from that of the Moon depending on its location. This has resulted in a sensible comparison of the timing above due to combined cycles of Sun and Moon.

2. Available Data

2.1. General

The main source of earthquake data for analysis for the first 30 years (since 1973) has been the USGS National Earthquake Information Centre (NEIC) database published on the Internet [9]. Subsequently, data have been collected from the European EMSC Last Quake website [10] as this provides more information on areas not covered in detail by USGS. In the analysis, only those prior events with magnitude greater than M6 have been selected for the Asia-Pacific and N/S America regions, starting at the first available year (1973) until the present. However, events of lesser magnitude M5+ have also been integrated in the analysis for Europe and Africa, as there are generally fewer larger M6+ events in the time period for this region.

Data provided includes Year, Month, Day, Time (hr. min. sec.) UTC, Latitude, Longitude, Magnitude, and Depth. Orbital data of the Moon and Sun have been obtained from JPL Horizons On-Line Ephemeris System [11].

2.2. NASA Ephemeris Data Collected

Date (UT) HR: MN, R.A. (a-app), DEC_(a-app), dRA*cosD, d(DEC)/dt, Azi_(a-app), Elev_(a- app), dAZ*cosE, d(ELV)/dt, ObsSub-LON, ObsSub-LAT, delta, deldot. This data is collected hourly for chosen observer reference sites as follows: Asia Pacific Zone—M8.9 Off N. Sumatra (Lat 3.3N, Lon 95.78E).

Asia Pacific Zone—Off N. Sumatra (Lat 3.3N, Lon 95.78E).

Americas—San Francisco. (Lat 37.78N, Lon 122.41W).

Europe & Africa—Rome. (Lat 41.87N, Lon 12.62E).

Philippines—Manila. (Lat 14.62N, Lon 121.0E).

2.3. NASA Ephemeris Data Definitions

- "R.A. (a-app), DEC_(a-app)," = Airless apparent right ascension and declination of the target center with respect to an instantaneous reference frame defined by the Earth equator of-dat (z-axis) and meridian containing the Earth equinox.
- "dRA*cosD, d(DEC)/dt," = The angular rate of change in apparent RA and DEC of the target. This is with respect to the non-inertial IAU76/80 Earth true equator and equinox of-date reference frame. d(RA)/dt is multiplied by the cosine of declination to provide a linear rate in the plane-of-sky. Units: ARCSECONDS PER HOUR.
- "Azi_(a-app), Elev_(a-app)," = Airless apparent azimuth and elevation of target center. Compensated for light-time, the gravitational deflection of light, stellar aberration, precession, and nutation. Azimuth is measured clockwise from North (0) → East (90) → South (180) → West (270) → North (360).
- Elevation angle is with respect to a plane perpendicular to the reference surface local zenith direction. TOPOCENTRIC ONLY. Units: DEGREES.
- "dAZ*cosE, d(ELV)/dt," = The rate of change of target center apparent azimuth and elevation(airless). d(AZ)/dt is multiplied by the cosine of the elevation angle. TOPOCENTRIC ONLY. Units: ARCSECOND PER MINUTE.
- "ObsSub-LON, ObsSub-LAT," = Apparent planetodetic longitude and latitude of the center of the target disc seen by the OBSERVER at print-time. Latitude is the angle between the equatorial plane and the line perpendicular to the reference ellipsoid of the body, so includes body oblateness. Positive longitude is to the EAST for this target. Cartographic system is given in the header. Units: DEGREES.
- "delta, deldot," = Apparent range ("delta", light-time aberrated) and range-rate ("delta-dot") of the target center relative to the observer. A positive "deldot" means the target center is moving away from the observer; negative indicates movement toward the observer. Units: AU and KM/S.

2.4. NASA Ephemeris Data Development

For prediction purposes, the data mentioned in section 2.2 have been downloaded as text files and then transferred into MS Excel spreadsheets for each of the above locations. This has been done at the start of each year for the subsequent annual period—first for the earth-lunar data (one set of daily data at 0:00 hrs only and one set of hourly data for 24 hrs. per day), then the same for earth-solar data.

Also, for historic (correlation) purposes, the data mentioned in section 2.2 have been downloaded as text files, then transferred into MS Excel spreadsheets for each of the above locations. This has been done at the start of each historic period of about 2 days close to the related historic event (one day before and 1 day after)—first for the earth-lunar data (one set of hourly data), then the same for earth-solar data. The reason for downloading 24 hours of data before and after the event is to enable an understanding of the event time in relation to the varying direction of travel of the heavenly objects relative to the terrestrial location of the event.

3. Analysis and Results

3.1. Analysis Based on Lunar and Solar Relationships

Because the tidal force of the Moon is more than twice as strong as that of the Sun, the tides follow the lunar day, not the solar day. It takes half a lunar day, on average 12 hours and 25 minutes, from one high tide to the next, so there are high and low tides nearly twice a day.

What causes the tidal forces? The Gravitational force is an attractive force that exists between all objects with mass; an object with mass attracts another object with mass; the magnitude of the force is directly proportional to the masses of the two objects and inversely proportional to the square of the distance between the two objects.

So that Force (F):

$F = g \times M1 \times M2/(D2 - D1)^2$—where g is the universal gravitational constant.

So, it can be considered that there is a gravitational attractive force between the Sun and the Earth as a whole (Fs) and another between the Earth and the Moon (Fm). The combined force of these two bodies can be computed as a vector force with components of distance, time and direction.

So, it would be expected that due to these attractive forces, the Moon would soon crash into the Earth and the Earth and Moon would a bit later crash into the sun.

But let us also consider the gravitational effect of the forces on the tectonic plates.

At any point on Earth, the plate on which one may be standing will be affected by the pull of the Sun and moon, which may vary in its combined direction and strength, and by the downward pull of the much closer mother Earth, which will be a more or less fixed amount and direction at that location. Thus, the combined force on the tectonic plate at one particular location will vary according to the location of the Sun and the moon, and to a much lesser extent even the solar planets and the (Milky Way) galaxy.

But again, the dynamic effects of the solar system should also be considered. Consider, for instance, that the Moon and the Sun are constantly in motion relative to one's location. Even though they may not actually have a course exactly through that location, assuming that they maintain a roughly regular orbit around each other, at almost any time they may be approaching and then receding. Thus, they will have an apparent acceleration towards and away from that point of reference. This relative acceleration (+ve./−ve.) is the result of a varying force in terms of magnitude and direction which acts also on the tectonic plate on which one may be standing.

These relative acceleration forces have the following main effects:

- Before moon-rise, there will be a relative downwards force; then around (within a few hours OF) moon-rise the force will tend to be more tangential to our location (from the East), and after moon-rise it will be more uplifting.
- As the Moon passes overhead, it will lose most of the tangential component, but this will increase again during moon-set, but in the opposite direction (from the West).

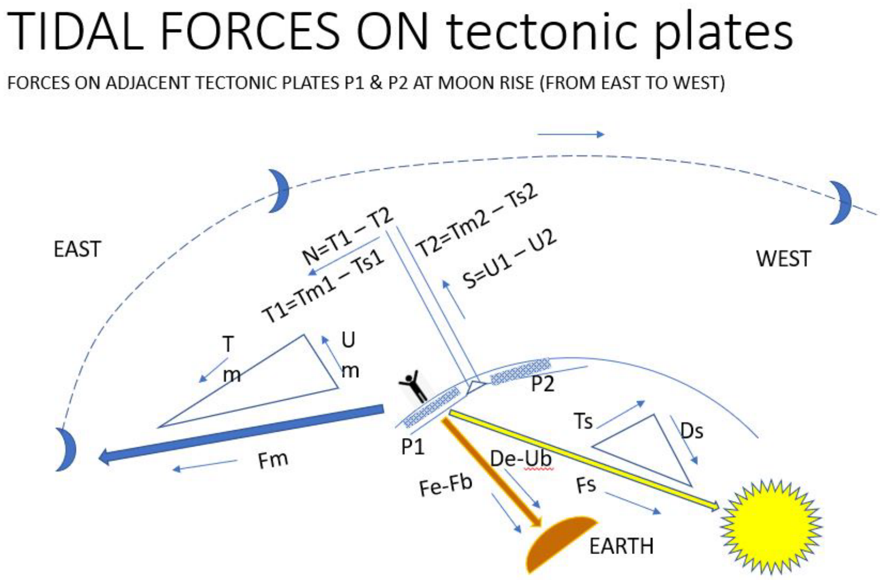

Figure 1. Dynamic forces on tectonic plates.

LEGEND	
P1 = Plate 1	Ds = Downward Force due to Sun
P2 = Plate 2	De = Downward Force due to Earth Gravity
Fe = Earth Gravitational Force	Ub = Upward Force due to Bouyancy
Fb = Bouyancy Force	N = Normal Force between Plates
Fm = Combined Force due to Moon	S = Shear Force (vertical) between Plates
Fs = Combined Force due to Sun	U1 = Net Vertical Force on Plate 1
Tm = Tangential Force due to Moon	U2 = Net Vertical Force on Plate 2
Ts = Tangential Force due to Sun	T1 = Net Tangental Force on Plate 1
Um = Upward force due to Moon	T2 = Net Tangential Force on Plate 2

The main effect of these forces will be to separate the tectonic plate on the side closest to the Moon (P1) from the more distant plate (P2). This will result in less force normal (N) to any N-S oriented (dip slip—normal or reverse) fault line and consequently less frictional resistance to slippage.

Of course, the lunar orbit is not always directly overhead as it has varying declination with respect to the meridian. This varying declination will result in transverse forces acting also on obliquely aligned tectonic boundary faults such N-W, S-E, N-E and S-W.

In **Figure 1**, it would be normal to find that T1—the tangential Force for Plate P1 would be greater than T2—the Tangential force for Plate P2, due to the closer proximity of the center of Plate P1 to the Moon during Moon rise.

While this difference can be considered small due to the relatively short distance between plate centers (say a few thousand kilometers compared to the Moon average 250,000 km), the Plate masses and inertia are huge and each time the Moon crosses the threshold, this will impart a nudge which will have a cumulative effect on accumulated boundary tensions.

3.1.1. Lunar Phase Effects and SYZYGY

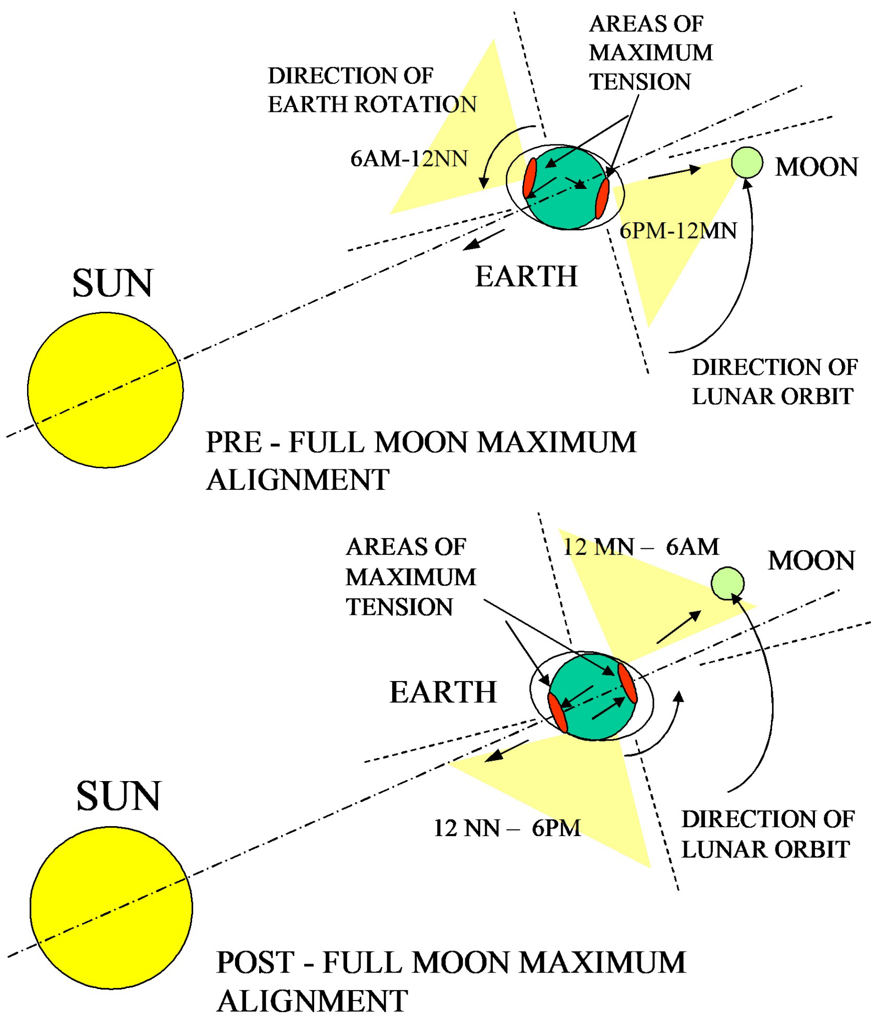

Figure 2. Effects of full Moon phase on the Earth's crust at times of day.

In **Figure 2**, a graphical representation of the Sun-Earth-Moon position during the Full Moon phase is illustrated, in which it should be remembered that the Moon is in orbit in an anticlockwise direction, looking down from above the North Pole and passes completely around Earth once every 29.53 days. However, the Earth itself is rotating about its slightly inclined axis also in an anticlockwise direction looking down from above the North Pole but with complete rotation once every 23 hrs and 50 minutes. Daily and hourly Lunar and Solar variations.

In order to understand more clearly the relation between Earth, Moon and Sun location, the author has recently evaluated substantial quantities of daily and hourly location data obtained from the "Horizons" website of Jet Propulsion Laboratory of California Institute of Technology and NASA.

Daily orbital data of the Moon were studied for the 53-year period from 1973 to the present and compared with the occurrence of major quakes in the Region. Data such as Right Ascension (RA) and Declination relate to the celestial sphere, while Azimuth and Elevation relate to global reference. These values vary substantially on an hourly basis so are not useful for daily analysis.

3.1.2. Hourly Lunar Variations

A more precise indication of earthquake timing can be gained by reference to hourly lunar orbit and in particular to the distance of the Moon from any potential earthquake zone on Earth and the rate of acceleration towards and away from this point.

Even if the forecast quake does not occur at or close to the maximum or minimum rate of change of range "deldot", there is a strong likelihood that another quake in the forecast location can follow at about 12 hours or 24 hours after the preceding quake.

One question, which may be asked, is whether this tendency for plate boundary activity is due to acceleration/deceleration of the Moon with respect to this point on Earth or due to the angle of approach/departure which tends to pull tectonic plates tangentially to Earth's surface, or more likely a combination of both.

The Moon is in a state of dynamic balance with the earth, so that in one direction the gravitational forces are pulling the two bodies together, while in the other the velocity of travel around the Earth results in radial acceleration with corresponding force of separation.

3.1.3. Lunar/Solar Hourly Direction and Acceleration Analysis

Hourly evaluation of vector direction and radial acceleration has been computed and results correlated against results of historic earthquakes over the last 53 years (*i.e.*, from 1973 to present). Thus, yearly tables have been produced for specific areas (Asia-Pacific, Americas, Europe & Africa, Philippines), which show the most likely earthquake occurrence location based on similar acceleration and combined direction vector as well as solar direction vector. The assumption has been made that the tidal influence of the Moon is about 2.21 times as strong as that of the Sun (value taken from available literature in the public domain). A tidal model has not been used, partly because the author does not have access to such, and secondly because the concept of the present paper is not suggesting that Earth tides (through friction) are responsible for many quakes, but rather that the tectonic plates themselves are pushed and pulled as largely monolithic structures directly by lunar and solar forces.

1) Analysis of NASA Ephemeris Daily Data

For predictions, the annual daily lunar and solar data sets are combined into one file to provide a daily combined eccentricity of orbit, which allows for an overall estimation of relative likelihood of an event occurring in particular regions, based on historic correlation with numbers of previous events at similar eccentricities. For Asia-Pacific, this has been broken down into 13 regions (N. Sumatra, S. Sumatra, W. Java, Surigao, Gensan, Manila, Baguio, Taiwan region, Kyushu, Hokkaido, Tokyo, E. Honshu, Kuril) and 5 levels (high, med-hi, medium, med-lo and low). The results of the daily analysis are not affecting the hourly analysis. Results of the daily analysis are not discussed in this paper, but may be used as a guide to estimation of likelihood of success of the hourly forecasts in related regions.

2) Analysis of NASA Ephemeris Hourly Data

For predictions, the annual hourly lunar and solar data sets are combined into one file to provide a daily combined estimate of directions of approach (for moon, Sun and overall), time of change of direction of approach and relative acceleration, which allows for an overall estimation of relative likelihood of an event occurring in particular location at a particular time (hour), based on historic correlation with numbers of previous events at similar directions of approach (for moon, Sun and overall), time of change of direction of approach and relative acceleration. The hourly Ephemeris downloaded data included in the combined table is for "Azi_(a-appr)_Elev.; dAZ*cosE; d(ELV)/dt; Ob-lon; Ob-lat; delta; deldot" - all as defined in 2.3 above (one set of 8 columns for lunar and one set of 8 columns for solar).

The combined lunar-solar files have been developed yearly for specific areas (Asia-Pacific, Americas, Europe & Africa, Philippines), starting in year 2005 for Asia-Pacific and 2012 for Americas and Europe-Africa.

The input variables are as follows:

a) Time (hour/day/month/year)

b) Location—names commonly used geographic names associated with historic earthquakes

c) Lunar and solar:

i) Azi_(a-app), Elev_(a-app), = Airless apparent azimuth and elevation of target center.

ii) dAZ*cosE, d(ELV)/dt, = The rate of change of target center apparent azimuth and elevation(airless). d(AZ)/dt is multiplied by the cosine of the elevation angle.

iii) ObsSub-LON, ObsSub-LAT, = Apparent planetodetic longitude and latitude of the center of the target disc seen by the observer.

iv) delta, deldot, = Apparent range ("delta", light-time aberrated) and range-rate ("delta-dot") of the target center relative to the observer.

Similarity thresholds:

a) For Asia Pacific and Americas input events are for M6+.

b) For Europe and Africa input events are for M5+ for low-frequency areas and M5.5+ for more frequent locations.

c) For all areas output forecasts are considered as M4+.

The choice of M4+ as a threshold is mainly based on a manageable quantity of data which would give a representative frequently updated spatio-temporal picture of the regional earthquake activity. Use of a lower threshold such as M3+ would result in much larger data volume and make it too time consuming to evaluate. The majority of high energy original quakes result in aftershocks of lower magnitude which decay to mainly M4+ level within a few hours. The question of whether one should consider every event—even the large ones—as aftershocks or whether they are in fact completely independent of the previous events, but just happen to propagate from the same locations has not yet been considered.

Geographic matching criteria:

Name of location as commonly used by main earthquake websites and within 200 km of the center thereof.

Rule for conversion of input data to forecast:

a) Computations on lunar downloaded data are then carried out in additional columns with headings as follows: "deldoubledot (km/sec^2); Max-Min deldot; dAZ*cosE—deg/day; d(ELV)/dt—deg/day; Vector sum—deg/day; Ω—rad/sec; delta—km; ä = relative accel (m/sec^2)—delta x Ω^2; ä (sign); Azi_(a-app)—global correction; direction vector (rad.); direction (cardinal)". Similar computations are then carried out on the downloaded solar data. Some results of the lunar and solar data are then combined as follows: "Azi_(a-appr)_Elev (lunar + solar/2.21); Azi_(a-app) combined—global correction; direction vector (rad.); direction (cardinal)".

b) The computation of relative acceleration is then adjusted to take account of the solar influence as follows: "Direction difference (between combined and lunar) radians; Solar Augmentation Factor; F = Corrected Solar Augmentation Factor (upper limit 2, lower limit 0.5); ä × F (combined acceleration)".

c) Computations are made on the exact hour for historic data and hourly for the forecast period, matching the lunar direction, the combined solar-lunar direction and the relative acceleration of the historic events with the current hourly criteria within an acceleration range of 0.3 m/sec^2.

3) Further Analysis to Provide Hourly Predictions

The results of the combined lunar-solar hourly spreadsheet are used as the basis of the annual hourly earthquake prediction sheet. Columns include:

Date	Time UST	Deldot km/sec	Direction Lunar	Ldir	Direction Solar	Sdir	Direction Combined	Cdir	Vector Accel

An algorithm (using MS Excel based macro) is provided that links the historic earthquakes solar-lunar combined data for comparison with the predicted hourly lunar-solar combined data. In order to do this a list of M6+ historic quakes in each region is compiled together with the related lunar-solar data which would have been in effect at the time of each original event. The list of historic earthquakes for each region is updated at the end of each calendar year—which typically adds about 20 to 30 events to each list so that there are presently in the order of 1000 events available for correlation in each region. Besides the solar-lunar data, the list includes information on the date/time UTC, name and latitude/longitude of each event.

4) Analysis—Hourly variation—some observations

The major earthquakes often appear to occur at times when the rate of travel of the Moon from the earthquake location ("deldot") is at or close to its maximum (+ve.) or minimum (−ve.) over the preceding twelve-and-a-half-hour period. This is actually the time of moonset (+ve.) or moonrise (−ve.). Hourly evaluation of solar/lunar vector direction and tangential acceleration has been computed and results correlated against results of historic earthquakes to determine the most likely events occurring at those locations. It has been observed that new events do not necessarily correlate precisely with similar directions and acceleration, so that a deviation range of +/−0.3 m/sec^2 from the predicted acceleration (which varies from −4.1 to −0.7 m/sec^2 and +0.7 to 3.8 m/sec^2) from the predicted acceleration has been allowed in the acceleration selection. The choice of this deviation range is practical as it gives a substantial but not overwhelming choice of earthquake location for strongly correlating hours. A smaller deviation would however provide too little information for forecast of most events.

5) Comment on the Tabulated Earthquake Analyses

With the exception of Aleutian Isles in extreme western parts of Alaska and S. Sandwich Isles and S. Shetland Isles, etc., in the south Atlantic, the majority of earthquakes in the N/S America region occur within a longitude band (between about 70˚W and 170˚W). The base line of the analysis passes through San Francisco with longitude approximately 122.4˚W.

With the exception of extreme Eastern parts of New Zealand, the majority of earthquakes in the Asia-Pacific region occur within a longitude band (between about 60˚E and 160˚E). The analysis has not attempted to forecast quakes in PNG, Solomons, Vanuatu, Tonga, Fiji, Oceania or Antarctica generally. The base line of the analysis passes through coastal North Sumatra with longitude approximately 95.8˚E.

The Europe/Africa region covers a longitude band (between about 40˚W and 60˚E). The selected base line of the analysis passes through Rome with longitude approximately 12.6˚E.

The analysis is based on correlation of data on an hourly basis. For each region, the lunar-solar dynamic characteristics are based on data related to a single point—such as the origin of the North Sumatra 2004 quake for Asia-Pacific data—so that there is a time lag between the forecast (results) and the actual event depending on the location (longitude) of the event—so for instance forecasts for Japan quakes will be 2 hours different, New Zealand will be 4 hours etc. Then there is the sensitivity to the lunar-solar force—as we are allowing a range of acceleration in order to provide more extensive coverage as we do not expect to be 100% accurate. This results in a reasonable time tolerance of 6 hours, which can be defined for the purpose of rigorous evaluation. This does not mean that some events may not occur outside this period, but only that for analytical purposes the more extreme events may be considered as misses.

6) General Results - Hourly Lunar-Solar Variations

About 33% of big quakes were found to occur within 1 hr. of moonset or rise (14% while the Moon is rising and 19% while setting). However, 11% occur about 1 hr. before moonset, which is nearly 3 times the expected average. At this moment, the tectonic plate to the east of a north-south boundary would be lifted up slightly at the same time as being pulled laterally to the west over the subducting plate located to the west of the boundary.

The rate of travel of the Moon relative to any point on the Earth's surface varies cyclically from a maximum of about 0.3 to 0.5 km/sec (waning) to a minimum of about −0.3 to −0.5 km/sec (waxing) over an approximately 24.8-hour cycle.

There is more likelihood of quakes occurring when the Sun and Moon are in the same sector (58%) rather than in apposition (42%). About 30% of quakes occur within 1 hour of a reversal in direction of acceleration of the combined solar and lunar acceleration vector with regard to the location of the quakes. This phenomenon appears to act like a jolt to the plate boundary, weakening transverse resistance, thus enabling lateral fault shear to occur.

It is found that earthquakes in particular zones are very sensitive to the exact positions and movement of Moon and Sun (less so). Thus, earthquakes in Taiwan region are most common a few hours before the Moon is setting with a WSW, WNW-W direction relative to that location with the East Asia Plate subducting under the Philippine Plate. This is believed to be because the main tectonic plate boundary lies in an NNE-SSW direction.

However, quakes in Indonesia (North/South Sumatra) tend to occur when the Moon is in the W direction a few hours after moonset or several hours after moonrise, when the Moon is towards the E. This is believed to be because the main tectonic plate boundaries in these regions lay in the N-S direction. For Java, a lunar NE-SW pull is more effective as the Java trench veers to the NW-SE direction locally.

3.2. Comparison of Predicted Information with Actual Events for Year 2023-2024

Although the lunar/solar dynamic model has been used to predict quakes on an hourly basis since about the year 2007, here is presented a summary of some analysis carried out on results for the one- year period between July 2023 and June 2024 (there is no particular reason for this period—other similar periods from

2014 to the present can be chosen). The July 2023-June 2024 forecasts were issued and archived before the earthquakes occurred. As normal practice, the author has for the last 11 years been uploading to a website available on public domain, hourly earthquake forecasts for the whole month ahead, before the start of each month for each region (AP, AM and EA). The results have been grouped into 3 regions—Asia-Pacific (AP), N/S America (AM) and Europe with Africa (EA). For details, see tabulations in supporting documents including "Summary of Daily Earthquake Events and Lunar Solar Dynamic Forecasts.xlsx" which includes a summary of results abstracted from tabulations in files: "com 2024 NS loc analysis.xlsm", "com 2024 AM loc analysis.xlsm", "com 2024_itloc analysis.xlsm".

3.2.1. Expectations for Results of Hourly Earthquake Analysis

In order to be meaningful a successful prediction of an earthquake must include prediction of the time of the event, the location and strength. In the case of hourly analysis by lunar-solar dynamics, the first item-time is the most easily accomplished, as forecasts are given on an hourly basis, so that for instance one might classify a successful prediction as when the event occurs within 6 hours of the forecast time.

Also, regarding location, it is suggested that a successful prediction would be for a location occurring within 200 km of the forecast location. (However, in the present analysis location is considered as being at or near a particular country or region of a country).

The model is based on data going back 50 years (or more in the case of Philippines separate analysis). Some (relatively few) of the original earthquakes used for training are known to be aftershocks as they were large events that occurred shortly after the larger main events but still had significant energy release. The inclusion of these for training was allowed because it is hypothesized that there may have been some lunar-solar influence affecting their occurrence at the time. It is acknowledged that this is an unproven assumption. The benefit for inclusion in the model is that the model will be more sensitive to larger events in the same area as those occurring previously—the main objective being to provide forecasts for large events.

The prediction of strength is more difficult to assess although clearly there would be limits of maximum probable strength based on the length and type of fault involved (but at present this is not an included parameter). For Asia-Pacific and N/S America all original events are of M6 or greater up to M9 and these prior events have occurred from 53 years ago until the present, so that forecast events based on these can vary significantly. At present there is not any automatic method of assessing forecast strength, so that all predicted events of M4+ with appropriate time and location (as above) are considered as being successful.

The method of evaluation is not sensitive to quake magnitude. The only significance noted is that a correlated result from a prior magnitude 7+ event is likely to affect a larger area than the exact location, so that for instance a prior M7+ event in Gensan might regularly result in an M5+ or M4+ in Sulawesi or Davao, while a prior M6+ in Gensan is more likely to result in M5+ or M4+ in Gensan and its closer neighborhood only. In order to assess expected quake magnitude, the author is using other factors such as temporal proximity and plate stress transfer. This is an ongoing work.

3.2.2. Results of Hourly Earthquake Analysis for July 2023-June 2024

Referring to the supporting document including "Summary of Daily Earthquake Events and Lunar Solar Dynamic Forecasts.xlsx"—this includes tables as follows:

- DAILY SUMMARY OF RESULTS OF HOURLY LUNAR-SOLAR DYNAMIC ANALYSIS
- MONTHLY SUMMARY OF RESULTS OF HOURLY LUNAR-SOLAR DYNAMIC ANALYSIS
- (INCLUDING% EXCLUDING BREAKDOWN OF QUAKES BY MAGNITUDE)
- MONTHLY PERCENT OF EFFECTIVE FORECASTS COMPARED WITH TOTAL FORECASTS
- MONTHLY PERCENT OF EFFECTIVE FORECASTS ASSOCIATED WITH ACTUAL QUAKE EVENTS
- MONTHLY TOTAL NUMBERS OF FORECASTS OF QUAKES OF M4+ BY REGION
- MONTHLY TOTAL WEIGHTED STRENGTH OF QUAKES OF M4+ BY REGION
- MONTHLY TOTAL NUMBER OF EVENTS OF M4+ BY REGION

1) Number of forecasts varied for each region, partly due to number of available historic data and partly due to selections of accuracy tailored to the available data. The total average number of automatically generated forecasts per day for each area was as follows: AP = 106, AM = 40, EA = 29.

Average monthly variation in daily numbers of forecasts AP (+19%/−22%), AM (+7%/−6%), EA (+18%/−8%).

2) Number of actual events greater than M4+ varied for each region. The total average number of recorded events per day for each area was as follows: AP = 14, AM = 11, EA = 2.6. From comparison with section 2.1 above, it can be seen that on average there were about 7.6 forecasts for every AP event, about 3.6 forecasts for every AM event, and about 11.2 forecasts for every EA event.

Variation in daily numbers of events

AP (Max 87, Min 3), AM (Max 29, Min 2), EA (Max 37, Min 0)

3) The overall annual percent of effective forecasts associated with actual quake events (%FET) was as follows: AP = 63%, AM = 76%, EA = 45%.

The daily percent of effective forecasts compared with events (%FET) varied from maximum 100% on some days for all regions to minima of 6% (AP), 8% (AM) and 0% (EA).

On a monthly basis compared with annual average, the max/min percent (FET%) varied as follows: AP (max/min) = 121%/68%, AM (max/min) = 111%/87%, EA (max/min) = 123%/51%.

An effective forecast (hit) on a given day is considered to be a forecast of an event of magnitude greater than M4 which is close to the actual event in terms of location and time (within six hours).

Concerning the year-long data from July 2023 to June 2024, for all regions the total forecasts, false alarms, misses and number of events have subsequently been included in the daily tabulation. Also, for AP the 0 forecast and 0 event column was added and combined with the false alarm to provide true negatives. The resulting Peirce Skill Score (PSS) values were mostly positive with average score of 0.17 and maximum of 0.52 and minimum of −0.44 and Hypergeometric Distribution (PMF) values have majority of days with value of 1 and average of all days for the year of 0.94. For AM and EA, the PMF had yearly average of 1.0 and 0.96 respectively. The negative PSS scores were mainly due to numerous not forecast aftershocks following large events which themselves may have been forecast. The aftershocks were not included in the true negatives but probably should have been.

4) The overall annual percent of effective forecasts compared with total forecasts (%FFT) was as follows: AP = 8%, AM = 22%, EA = 4%.

From the above, it is seen that less than 25% of alarms correspond to an earthquake event on an average day. However, the accuracy of the alarms given is sufficient to conform to a larger percentage of the events—so the information on the majority of events is contained within the alarms. In order to improve accuracy, it is then a matter of filtering these alarms to decide which are going to be effective and provide a hit, or not. This can be done by knowledge of other criteria such as recent history of events in the area, cumulative effect of previous forecasts, application of lunar trends, etc.

The percent of effective forecasts compared with total forecasts (%FFT) varied from maximum daily of 45% (AP), 57% (AM) and 23% (EA) to minimum daily of 1% (AP), 3% (AM) and 0% (EA).

On a monthly basis compared with the annual average, the max/min percent (FFT%) varied as follows: AP (max/min) = 164%/73%, AM (max/min) = 110%/92%, EA (m ax/min) = 130%/65%.

5) Comparison of forecasts with events for less frequent earthquake locations

Apart from the overall percentages indicated in section 2.1 to 2.4 above, there are many cases where results clearly indicate a correspondence between forecasts and subsequent actual events such as in **Table 1**, where it can be seen that these events are relatively unusual. As in several cases there is only one event occurring at the particular location per year, but even so a correct forecast was achieved to within a few hours.

False-Alarm rate and Missed Events have been included in **Figure A1** and analysis to determine success and accuracy, including Peirce Skill Score (PSS) and Hypergeometric Distribution (PMF) have been added. The results for **Figure A1** are variable, showing significance for 83% (AP), 33% (AM) and 50% (EA) on a daily basis, but when hourly accuracy is considered, the significance is good for 100% (AP), 67% (AM) and 83% (EA).

Table 1. List of unusual events with clear connection to forecasts.

Region	Date	Forecast location		Forecasts	Event location	Event		Time (hrs)	Events	Number of hits	Average
		Name	Time (hrs)	No. in Year	Name	Mag.	Time (hrs)	difference	No. in Year	Linked Events	time hrs
AP	7/1/2023	Phils (Leyte)	07 AM	24	Phils (Leyte)	M4.9	05 AM	2	20	1	2
AP	7/16/2023	Meghalaya 23 M7+	17 PM	30	India, Meghalaya	M4.3	14 PM	3	3	1	3
AP	8/13/2023	Batanes Isles	01 AM	11	Phils (Batan Isles)	M5.4	02 AM	1	4	1	1
AP	8/17/2023	Phils (Lanao del Sur)	10 AM	24	Phils (Lanao del Sur)	M4.3	17 PM	9	1	1	9
AP	9/17/2023	S. Qinghai	00 AM	29	S. Qinghai	M4.4	02 AM	2	5	1	2
AP	4/14/2024	N. Qinghai	21 PM	38	N. Qinghai	M4.9	18 PM	3	2	1	3
AM	12/24/2023	Off Washington	21 PM	63	Washington Olympic Peninsula	M4.0	15 PM	6	4	1	6
AM	12/25/2023	Puerto Rico	04 AM	42	Puerto Rico	M4.4	17 PM	13	18	1	13
AM	1/6/2024	N of Honduras	08 AM	72	Off Honduras	M4.5	21 PM	13	8	1	13
AM	3/27/2024	W Brazil	15 PM	179	W Brazil (Acre)	M4.0	14 PM	1	6	2	0.5
AM	6/3/2024	Hawaii	01 AM	20	Hawaii	M4.1	07 AM	6	9	1	6
AM	6/23/2024	Off Venezuela (Sucre) M7.3	02 AM	84	Venezuela (Sucre)	M6.1	04 AM	2	20	2	2.5
EA	7/4/2023	Mozambique	19 PM	197	Mozambique Channel	M4.8	17 PM	2	1	1	2
EA	9/30/2023	NE Morocco M5.1	07 AM	150	Morocco	M4.0	08 AM	1	10	3	3.67
EA	11/29/2023	Azerbaijan	14 PM	123	Azerbaijan	M4.5	16 PM	3	10	4	7.25
EA	1/13/2024	Adriatic Sea (Albania)	17 PM	224	Albania	M4.5	23 PM	7	3	1	7
EA	2/19/2024	N. Bosnia & H M6	18 PM	225	Bosnia & Herzegovina	M4.2	08 AM	10	5	1	10
EA	6/27/2024	France	07 AM	56	France-Germany Bdr.	M4.2	01 AM	6	2	1	6

LIST OF EVENTS WITH CLEAR CONNECTION TO FORECAST
(YEAR - JULY 2023 - JUNE 2024)

3.3. Comparison of Predicted Information with Actual Events for Other Periods

Besides the above review of the recent period in 2023-24, for interest some relatively successful forecasts have been selected for larger events in recent years such as in the table for Europe/Africa Year 2025 - M6+ below in **Table 2**, also the table of Events of Larger Magnitude (M7+) for Americas in Years 2019-2025 below in **Table 3** and the table of Events of Larger Magnitude (M7.5+) for Asia-Pacific in Years 2011-2025 below in **Table 4**

From the above-mentioned 3 regional tables of large events, it can be seen that in almost every case there is at least one link to an hourly forecast nearby within the 24-hour period surrounding the event. For many events there were considerable numbers of forecasts for the event location on the same day. In fact, many of the forecasts for the M7+ tables were associated with previous M7+ events.

Table 2. List of events of larger magnitude (M6+) for Europe and Africa in Year 2025.

REGION	DATE	LOCATION	OTHER FORECAST	Hourly Forecast (UTC)	Actual (UTC)	Magnitude
EA	14-Feb-25	EC. Ethiopia		18 PM	20 PM	M6.0
EA	10-Mar-25	Jan Mayen Island		19 PM	03 AM	M6.5
EA	28-Mar-25	C. Mid-Atlantic Ridge		2 AM, 8 AM	1 AM, 17 PM	M6.1, M6.6
EA	3-Apr-25	Reykjanes Ridge		6-Apr 10 AM	14 PM	M6.9
EA	23-Apr-25	W. Türkiye		11 AM	10 AM	M6.2
EA	13-May-25	E. of Crete	Greece, Crete	GC: 6 AM, 14-May 7 AM	23 PM	M6.0
EA	22-May-25	NE. of Crete	Greece, Crete	GC: 10 AM	2 AM	M6.2
EA	30-May-25	SW. of Africa	S. of Africa	S.o.A.: 01 June 3 AM	6 AM	M6.2
EA	25-Jun-25	S. Mid-Atlantic Ridge		12 June 12 PM	22 PM	M6.2
EA	10-Aug-25	W. Türkiye		8 AM	17 PM	M6.1
EA	27/10/2025	W. Türkiye	CW. Türkiye, NW Türkiye	CWT 14 PM, NWT 16 PM	21 PM	M6.1
EA	2-Nov-25	C. Afghanistan	W. Afghanistan	WA.: 5-Nov 12 PM	20 PM	M6.3

MAGNITUDE COMPARED WITH ACTUAL OCCURRENCE FOR EUROPE & AFRICA - Year 2025

Table 3. List of events of larger magnitude (M7+) for Americas in Years 2019-2025.

REGION	YEAR	DATE	LOCATION	OTHER FORECAST	Hourly Forecast (UTC)	Actual (UTC)	Magnitude
AM	2025	8-Feb-25	Cayman Isles		6 Feb-01 AM	23 PM	M7.1
AM	2025	2-May-25	Drake Passage	S. Pacific-Antarctic	S.P-A 12 PM	13 PM	M7.4
AM	2025	16-Jul-25	Alaska Peninsula	Gulf of Alaska	AP -18 Jul 7 AM, GoA 14 PM	20 PM	M7.3
AM	2025	22-Aug-25	Drake Passage	S. Pacific-Antarctic	S.P-A 21 PM	02 AM	M7.5
AM	2025	10-Oct-25	Drake Passage	S. Pacific-Antarctic	DP -11 Oct 7 AM, S. P-A 10 Oct - 9 AM, 12 PM	20 PM	M7.7
AM	2024	28-Jun-24	Coastal S Peru	C Peru, S Peru	CP-5 AM, 29-Jun 6 AM, SP 29-Jun 12 PM	6 AM	M7.2
AM	2024	19-Jul-24	NC Chile (Antofagasta)	Pacific (W of NC Chile)	P (WNC), 12 PM, 13 PM, 18 PM	1 AM	M7.4
AM	2023	16-Jul-23	Alaska Peninsula	Gulf of Alaska	AP -20 Jul 8 AM, GoA 13 PM	07 AM	M7.4
AM	2022	26-May-22	S Peru		9 AM, 6 PM, 23 PM	11 AM	M7.2
AM	2021	25-Jan-21	S. Shetland Isles	S. Sandwich Isles	S. San. I 3 AM	00 AM	M7.1
AM	2021	29-Jul-21	Alaska Peninsula	Gulf of Alaska	AP -09 Aug 7 AM, GoA 14 PM	06 AM	M8.2
AM	2021	12-Aug-21	S. Sandwich Isles		13-Aug, 00 AM, 13 PM	19 PM	M7.5

Continued

AM	2021	14-Aug-21	Alaska Peninsula	Gulf of Alaska, S of Alaska	GoA 11 AM, 15 PM, SoA 23 PM	12 PM	M7.0
AM	2021	14-Aug-21	Haiti		No forecast for Haiti	12 PM	M7.2
AM	2021	22-Aug-21	S. Sandwich Isles		15 PM, 23-Aug 2 AM	22 PM	M7.0
AM	2021	8-Sep-21	S. Mexico (Guerrero)	Mexico (Pueblo)	SM (G) 9-Sep 10 AM, M (P) 20 PM, 7-Sep 19 PM	2 AM	M7.0
AM	2021	28-Nov-21	N. Peru	Pacific (W of N Peru)	PWN 7 AM, 8 AM	11 AM	M7.5
AM	2020	23-Jun-20	S. Mexico (Oaxaca)	S.M. Guerrero, S.M. Jalisco	SM.G 10 AM, SM.J 12 PM (x2), SM 18 PM, 21 PM	15 PM	M7.4
AM	2020	22-Jul-20	Alaska Peninsula	Gulf of Alaska, Alaska (Anchor)	GoA 16 PM, A (An) 21-Jul 20 PM	6 AM	M7.8
AM	2020	19-Oct-20	S of Alaska	Gulf of Alaska,	GoA 16 PM, 20 PM	21 PM	M7.5
AM	2019	22-Feb-19	Peru-Ecuador Bdr.	Ecuador, S Peru	E. 00 AM, 02 AM, SP. 6 AM, 7 AM, 10 AM	22 PM	M7.5
AM	2019	1-Mar-19	S. Peru		14 PM (x2)	9 AM	M7.0
AM	2019	26-May-**19	N. Peru		3 AM	8 AM	M8.0
AM	2019	6-Jul-19	S. California	Baja	S.C. 14 PM, Baja 21 PM, 23 PM, 5-Jul 22 PM	3 AM	M7.1

LIST OF FORECAST EVENTS OF LARGE MAGNITUDE
COMPARED WITH ACTUAL FOR AMERICAS - 7 Years

Table 4. List of Events of Larger Magnitude (M7.5+) for Asia-Pacific in Years 2011-2025.

REGION	YEAR	DATE	LOCATION	OTHER FORECAST	Hourly Forecast (UTC)	Actual (UTC)	Magnitude
AP	2025	28-Mar-25	Myanmar		1 AM, 2 AM, 3 AM, 14 PM, 21 PM, 22 PM	6 AM	M7.7
AP	2025	29-Jul-25	Kamchatka		3 AM, 15 PM, 23 PM	23 PM	M8.7
AP	2025	18-Sep-25	Kamchatka		4 AM, 5 AM, also on 19th Sep 4 AM, 5 AM	19 PM	M7.8
AP	2025	8-Dec-25	NE of Honshu	E. Honshu	2 AM, 3 AM, 4 AM, 9 AM, 14 PM, 15 PM, 16 PMx2, 17 PM, 22 PM	14 PM	M7.6
AP	2024	1-Jan-24	W. Honshu	S. Honshu	SH. 6 AM	7 AM	M7.5
AP	2023	9-Jan-23	Kep. Babar	Timor	T: 12 PM, 13 PM	18 PM	M7.6
AP	2023	2-Dec-23	S. Surigao	Surigao	S: 21 PM	15 PM	M7.5
AP	2020	25-Mar-20	E of Kuril	Kuril	K: 9 AM, 14 PM, 17 PM, 24-Mar-15 PM (x 6)	3 AM	M7.5
AP	2018	28-Sep-18	Sulawesi		3 AM, 4 AM, 10 AM, 13 PM, 14 PM, 15 PM	10 AM	M7.5
AP	2017	18-Jul-17	Komandorskiye	Kuril	Kuril - 4 AM, 7 AM, 19 PM, 22 PM	00 AM	M7.7
AP	2016	2-Mar-16	Off SW Sumatra	S. Sumatra, N. Sumatra	SS: 14-15 PM, 19-22 PM, NS:00 AM, 3-6 AM, 13 PM, 22 PM	13 PM	M7.8
AP	2016	29-Jul-16	N. Marianas	Marianas	M: 02 AM, 13 PM	21 PM	M7.7
AP	2016	13-Nov-16	S. New Zealand	N. New Zealand	S.NZ 14-Nov 22-23 PM, N.NZ: 10 AM, 11 AM	11 AM	M7.9

Continued

AP	2015	25-Apr-15	Nepal		26-Apr 9 AM, 27-Apr 8 AM	6 AM	M7.8
AP	2015	30-May-15	Bonin Isles	SE Ryukyu	SER: 9 AM	11 AM	M7.8
AP	2015	26-Oct-15	Hindu-Kush	N. Pakistan	H-K: 25-Oct 22 PM, NP: 13 PM	9 AM	M7.5
AP	2013	16-Apr-13	Iran-Pakistan Bdr.	Pakistan	P: 6 AM	11 AM	M7.8
AP	2013	24-May-13	Sea of Okhotsk	Kuril	K: 3 AM, 4 AM, 19 PM, 20 PM, 23 PM	6 AM	M8.3
AP	2013	24-Sep-13	SW. Pakistan	N. Pakistan	NP: 12 PM, 15 PM	11 AM	M7.7
AP	2012	11-Apr-12	N. Sumatra	Simeulue	NS: 00 AM, 15 PM 21 PM, 23 PM, S:13 PM-14 PM	9 AM, 11 AM	M8.6, M8.2
AP	2012	14-Aug-12	Sea of Okhotsk	Kuril	SO: 15-Aug 01 AM, K:13-Aug 19 PM-22 PM	3 AM	M7.7
AP	2012	31-Aug-12	Phils (Surigao)	Moro Gulf	MG: 00 AM 6 AM, 11 AM, 12 PM,	13 PM	M7.6
AP	2011	11-Mar-11	E. Honshu		4 AM, 5 AM, 12 PM (X2)	6 AM	M8.9

LIST OF FORECAST EVENTS OF LARGE MAGNITUDE COMPARED WITH ACTUAL FOR ASIA PACIFIC - M7.5+

In these tables, the column headed "other forecast" refers to forecasts of nearby areas or similar areas under a different name.

It is notable that for Europe and Africa the strength of larger events is mostly confined to M6+ and that relatively few forecasts were associated with these events.

The strongest quakes were noted in the Asia-Pacific region, so only those of M7.5+ have been shown. Most notable of these of course was the M8.9 East Honshu event of 11 March 2011, for which the algorithm had a total of 4 hourly forecasts on the same day. However, there were also from 2 to 4 forecasts on several days preceding this event, including 9th March when an M7.2 event was recorded, so that it is not possible to claim justification of a forecast for the extreme severity of this event.

In several cases (about one third) the forecast events have related to prior events of large magnitude, such as M7+ in Asia-Pacific and Americas and M6+ in Europe and Africa. However, this M7+ precursor was not the case in the majority of large events, so that specific forecasting of major events remains a challenge.

4. Discussion on Results of Hourly Earthquake Analysis

The results are grouped in 3 regions—Asia-Pacific (AP), N/S America (AM) and Europe with Africa (EA). From the preceding results in all criteria, the most successful predictions have consistently been for the N/S Americas (AM), followed by Asia-Pacific (AP), then some way behind by Europe & Africa (EA). It is postulated that the main reasons for this are as follows:

1) The N/S America region has a much higher percentage of tectonic plate boundaries with close to North-South orientation—these include the east boundary of the Pacific Plate, the east boundary of the Nazca plate, the east boundary of the Coco plate, the west boundary of the South American plate. The majority of faults along the north-south alignments are thrust faults which are more susceptible to Earth's east-west tidal rotation and the majority of earthquakes in these

regions are along these lines. See Figure 3—AM for Americas—left side vertical ellipse.

2) The Europe-Africa region has most earthquakes occurring along the southern boundary of the Eurasian Plate, which is oriented in an east-west direction and contains mainly thrust/strike faults which are not so directly susceptible to the Earth's east-west tidal rotation. See Figure 3—for EA—central regions—horizontal ellipses.

3) The Asia-Pacific region includes both a substantial number of north-south oriented plate boundaries (Philippine Plate and Pacific Plate-west) and a substantial number of more east-west oriented plate boundaries—Himalayas and Java trench—so is intermediate with regard to direct tidal effects. See Figure 3—for AP—right side—horizontal and vertical ellipses.

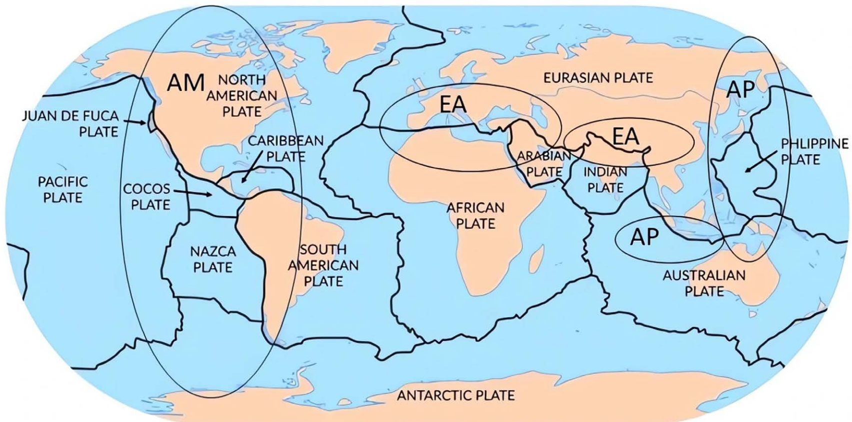

Figure 3. Comparison of alignment of tectonic boundaries globally.

5. Conclusions and Recommendations

5.1. Conclusions-Summary

The use of lunar and solar dynamics in a simplified model such as presented herein provides a convenient and widely accessible tool for estimation of future earthquake occurrence. While the results are far from perfect, they do provide a ray of hope that with additional refinement there will be improvement to a level that will be useful in providing early warning to susceptible areas.

It is considered that the use of this method in combination with filtration based on other factors is likely to provide a reasonable forecast model in the near future. It would most likely be possible to use an earth-tide model to provide similar correlation with historic events, but it is not so clear how such models could be adapted.

5.2. Recommended Improvements

One of the improvements that can be made, but with some extra work, is the forecasting connected with specific fault zones rather than generalized geographical regions. A second modification would take account of the varying distance of the Moon from Earth (not yet fully incorporated).

The accuracy of the forecasts also relies to a large extent on the completeness of the base data—so that improvements to this should provide better results. Although it is clear that older historic events have a lesser impact than more recent events, they are still important. A study of the actual decay of sensitivity to previous events over time would be beneficial and results could be incorporated into the model.

The author is also working on several different filtration techniques, such as understanding stress transfer across plate boundaries and effects of lunar orbit eccentricity.

From the introduction, it is seen that machine learning has shown some promising potential for improvements in earthquake forecasting. It would seem that a next step would be to integrate machine learning with the lunar solar dynamic parameters to provide a global analysis for short-term prediction of earthquakes with considerably improved accuracy. This hybrid analytical machine learning approach would require the supervisory introduction of successfully adopted analytical formulae and proposed variations to be optimized by machine learning.

Conflicts of Interest

The author declares no conflicts of interest regarding the publication of this paper.

References

[1] Geller, R.J. (1997) Earthquake Prediction: A Critical Review. *Geophysical Journal International*, **131**, 425-450. https://doi.org/10.1111/j.1365-246x.1997.tb06588.x

[2] Cochran, E.S., Vidale, J.E. and Tanaka, S. (2004) Earth Tides Can Trigger Shallow Thrust Fault Earthquakes. *Science*, **306**, 1164-1166. https://doi.org/10.1126/science.1103961

[3] Kossobokov, V.G. (2006) Testing Earthquake Prediction Methods: The West Pacific Short-Term Forecast of Earthquakes with Magnitude MwHRV ≥ 5.8. *Tectonophysics*, **413**, 25-31. https://doi.org/10.1016/j.tecto.2005.10.006

[4] Moghadamnejad, A., Moghaddasi, M.A., Hamidia, M., Mohammadi, R.K. and Zare, M. (2026) Ranking Earthquake Prediction Algorithms: A Comprehensive Review of Machine Learning and Deep Learning Methods. *Soil Dynamics and Earthquake Engineering*, **200**, Article ID: 109740. https://doi.org/10.1016/j.soildyn.2025.109740

[5] Zhang, Z. and Wang, Y. (2023) A Spatiotemporal Model for Global Earthquake Prediction Based on Convolutional LSTM. *IEEE Transactions on Geoscience and Remote Sensing*, **61**, 1-12. https://doi.org/10.1109/tgrs.2023.3302316

[6] Yousefzadeh, M., Hosseini, S.A. and Farnaghi, M. (2021) Spatiotemporally Explicit Earthquake Prediction Using Deep Neural Network. *Soil Dynamics and Earthquake Engineering*, **144**, Article ID: 106663. https://doi.org/10.1016/j.soildyn.2021.106663

[7] Astuti, W., Akmeliawati, R., Sediono, W. and Salami, M.J.E. (2014) Hybrid Technique Using Singular Value Decomposition (SVD) and Support Vector Machine (SVM) Approach for Earthquake Prediction. *IEEE Journal of Selected Topics in Applied Earth Observations and Remote Sensing*, **7**, 1719-1728. https://doi.org/10.1109/jstars.2014.2321972

[8] Rafiei, M.H. and Adeli, H. (2017) NEEWS: A Novel Earthquake Early Warning Model Using Neural Dynamic Classification and Neural Dynamic Optimization. *Soil*

Dynamics and Earthquake Engineering, **100**, 417-427. https://doi.org/10.1016/j.soildyn.2017.05.013

[9] USGS National Earthquake Information Centre (NEIC). Search Earthquake Catalog. https://earthquake.usgs.gov/earthquakes/search/

[10] Centre Sismologique Euro-Méditerranéen: Euro-Mediterranean Seismological Centre (CSEM:EMSC)—Latest Earthquakes. https://www.emsc-csem.org/

[11] Horizons Systems—Download Ephemerides—Jet Propulsion Laboratory of California Institute of Technology—NASA JPL Solar System Dynamics. https://ssd.jpl.nasa.gov/horizons/app.html#/

Appendix

Region	Date	Forecast location		FALSE	Missed	TRUE	PSS	PE	PF	Joint P	Success	Success	FA	ME	Hypergeometric.Dist	
		Name	Time (hrs)	Alarms	Events	Negatives	daily	in day	in day	in day	P daily	P hourly	P	P	H.D - daily	H.D - hourly
AP	7/1/2023	Phils (Leyte)	07AM	23	19	323	(0.02)	5.5%	6.6%	0.36%	0.27%	3.3%	6.3%	5.2%	0.62	0.99
AP	7/16/2023	Meghalaya 23 M7+	17PM	29	2	334	0.25	0.8%	8.2%	0.07%	0.27%	2.2%	7.9%	0.5%	0.98	1.00
AP	8/13/2023	Batanes Isles	01AM	10	3	352	0.22	1.1%	3.0%	0.03%	0.27%	6.6%	2.7%	0.8%	1.00	1.00
AP	8/17/2023	Phils (Lanao del Sur)	10AM	23	-	342	0.94	0.3%	6.6%	0.02%	0.27%	0.7%	6.3%	0.0%	1.00	1.00
AP	9/17/2023	S.Qinghai	00AM	28	4	333	0.12	1.4%	7.9%	0.11%	0.27%	3.3%	7.7%	1.1%	0.95	1.00
AP	4/14/2024	N. Qinghai	21PM	37	1	327	0.40	0.5%	10.4%	0.06%	0.27%	2.2%	10.1%	0.3%	0.99	1.00
AM	12/24/2023	Off Washington	21PM	62	3	300	0.08	1.1%	17.2%	0.19%	0.27%	1.1%	16.9%	0.8%	0.86	0.99
AM	12/25/2023	Puerto Rico	04AM	41	17	307	(0.06)	4.9%	11.5%	0.56%	0.27%	0.5%	11.2%	4.6%	0.36	0.69
AM	1/6/2024	N of Honduras	08AM	71	7	287	(0.07)	2.2%	19.7%	0.43%	0.27%	0.5%	19.4%	1.9%	0.51	0.79
AM	3/27/2024	W Brazil	15PM	177	4	183	(0.16)	1.6%	48.9%	0.80%	0.55%	26.2%	48.4%	1.1%	0.36	1.00
AM	6/3/2024	Hawaii	01AM	19	8	338	0.06	2.5%	5.5%	0.13%	0.27%	1.1%	5.2%	2.2%	0.92	0.99
AM	6/23/2024	Off Venezuela (Sucre) M7.3	02AM	82	18	264	(0.14)	5.5%	23.0%	1.25%	0.55%	5.2%	22.4%	4.9%	0.12	0.99
EA	7/4/2023	Mozambique	19PM	196	-	169	0.46	0.3%	53.8%	0.15%	0.27%	3.3%	53.6%	0.0%	1.00	1.00
EA	9/30/2023	NE Morocco M5.1	07AM	147	7	209	(0.11)	2.7%	41.0%	1.12%	0.82%	5.4%	40.2%	1.9%	0.36	1.00
EA	11/29/2023	Azerbaijan	14PM	119	6	237	0.07	2.7%	33.6%	0.92%	1.09%	3.6%	32.5%	1.6%	0.78	1.00
EA	1/13/2024	Adriatic Sea (Albania)	17PM	223	2	140	(0.28)	0.8%	61.2%	0.50%	0.27%	0.9%	60.9%	0.5%	0.33	0.92
EA	2/19/2024	N.Bosnia & H M6	18PM	224	4	137	(0.42)	1.4%	61.5%	0.84%	0.27%	0.7%	61.2%	1.1%	0.07	0.62
EA	6/27/2024	France	07AM	55	1	309	0.35	0.5%	15.3%	0.08%	0.27%	1.1%	15.0%	0.3%	0.98	1.00

STATISTICAL ANALYSIS OF EVENTS WITH CLEAR CONNECTION TO FORECAST (YEAR - JULY 2023 - JUNE 2024)

Figure A1. Analysis of unusual events with clear connection to forecasts.